Final Research Report

Federal Award Number: NIJ 2020-75-CX-0015

Project Title: Determining Fracture Timing from Microscopic Characteristics of Cortical Bone

Principal Investigator: Natalie R. Langley, PhD
Associate Professor of Anatomy
Department of Laboratory Medicine and Pathology
Mayo Clinic Arizona
13400 E. Shea Boulevard, Scottsdale, AZ 85259
Phone: 480-301-6164
Email: langey.natalie@mayo.edu
ORCID: 0000-0002-9332-3313

Award Recipient Organization: Mayo Clinic Arizona
Institutional Official (AOR): Craig Stewart
13400 E. Shea Boulevard
Scottsdale, AZ 85259
DUNS:

Project Period: 01/01/2021-06/30/2023

Award Amount: $463,595.00

Keywords: Forensic anthropology, skeletal trauma, scanning electron microscopy, bone histology, osteon, collagen

Table of Contents

Project Summary

Determining if an injury occurred before death (antemortem), around the time of death (perimortem) or after death (postmortem) is typically straightforward if the soft tissues are present but becomes more challenging as remains skeletonize. Bone may maintain elasticity for days, weeks, even months after death depending on environmental circumstances. Numerous studies [1-9] have demonstrated that the current practice of examining macroscopic fracture characteristics is limited and unreliable for determining fracture timing with scientific certainty, particularly during the transitional period between elastic and brittle bone. The inability to make this distinction may mean cause and/or manner of death are undetermined, and families are denied justice and closure for the untimely loss of their loved ones. This research leverages the multidisciplinary expertise of three academic research centers (Mayo Rochester, Mayo Arizona, Arizona State University) to employ an innovative, controlled experimental design and derive baseline data on the microscopic characteristics of perimortem and postmortem fractures.

Major Goals and Objectives

The study's main goal is to characterize microscopic features able to discern the timing of traumatic events more effectively than current methods (i.e., macroscopic observations of fracture patterns). Three interrelated specific aims address this primary goal:

1. Utilize histochemical analysis to assess the amount of collagen present in bone specimens of varying postmortem intervals.
2. Use scanning electron microscopy to identify micro-morphological features of experimentally induced peri- and postmortem fracture surfaces.

3. Correlate the results from Aims 1 and 2 to establish quantitative criteria to determine fracture timing relative to bone elasticity.

Research Questions

The main research question is: do microscopic fracture surface features provide more sensitive data about the timing of bone injuries than macroscopic fracture patterns? Secondary questions surround the nature of postmortem changes in the organic materials in bone's extracellular matrix (e.g., collagen and hydrophilic glycosaminoglycans) and the histological structure and integrity of osteons. As collagen and water content decrease over time, bone becomes less elastic and more brittle, and these material changes affect fracture morphology. We hypothesized postmortem changes in bone's biomechanical properties do not manifest macromorphologically in the early stages of bone's transition from an elastic to brittle material. Therefore, this research aimed to determine when postmortem changes in bone's material properties manifest microscopic indicators of the timing of fracture events.

Research Design and Methods

The research design was structured to control as many variables as possible in an experimental setting. While this may not mimic actual environmental conditions, the controls provide greater power and experimentally-sound baseline data. The following variables were controlled in this experiment: temperature, fracture mechanism (impact direction and energy), and bone type. Thirty-seven unembalmed, defleshed human femoral shafts were harvested from males (n=18) and females (n=2) aged 33–81 years (mean=61, standard deviation=16 years) with the periosteum intact. Vital statistics were recorded, including antemortem height, weight, medical diagnoses, and cause of death. Femoral shaft sections ranged from 155 to 194 mm in length (mean=179.3 mm), and body mass index ranged from 21.6 to 27.9 (mean=25.6). The bones were stored at −22°C and thawed at ambient temperature (20°C)

for two days prior to experimental treatment. Eight femora were used as the perimortem sample, and 29 femora were placed in a Thermo Fisher Heratherm gravity convection oven at either 27°C or 37°C to simulate seven target postmortem intervals while remaining below the temperature threshold at which collagen denatures (58°C) [10].

Postmortem interval (PMI) was calculated in Accumulated Degree Hours (ADH). As an example, a bone placed in a 25°C oven requires 40 hours to accumulate 1000 degrees (1000/25=40). We obtained data from perimortem fractures and seven targeted postmortem time points ranging from 1000 to 40,000 Accumulated Degree Hours (target ADH). Actual (observed) ADH was calculated for each sample factoring in storage and transport conditions data from donor facilities, as well as time and temperature data during thawing, oven heating, and transit between Mayo Clinic and Arizona State University for fracture experiments. Temperatures below 0°C were not included in ADH calculations. Table 1 shows the target ADH for sample cohorts and the observed ADH after incorporating storage, thaw, and transport data. Observed ADH for the unheated (perimortem) samples was 250, while heated samples ranged from 1145 to 40,600 ADH. A data logger was used to monitor and record temperature and humidity. Temperature remained constant, while humidity varied from 20% to 83% (mean=41.7%, SD=15.9%) in the 27°C experiments and between 15% and 66% (mean=26.9%, SD=6.6%) in the 37°C experiments.

This resource was prepared by the author(s) using Federal funds provided by the U.S. Department of Justice. Opinions or points of view expressed are those of the author(s) and do not necessarily reflect the official position or policies of the U.S. Department of Justice.

TABLE 1. Accumulated Degree Hours (ADH). Observed ADH incorporates data from storage conditions, thawing, heating (for postmortem samples), and transport time to ASU for fracture experiments.

	Experimentally Induced Accumulated Degree Hours							
Target ADH	Approximate calendar days		Time in oven (hours)		Number of samples		**Observed ADH**	
	27C	**37C**	**27C**	**37C**	**27C**	**37C**	**27C**	**37C**
0	0	0	0	0	4	4	250	250
1000	1.7	1.2	40	28.6	2	2	1145	1240
1500	2.5	1.8	60	42.9	2	2	1760	1547
3000	5.0	3.6	120	85.7	2	2	3267	3010
6000	10.0	7.1	240	171.4	2	2	6288	6345
8000	13.3	9.5	320	228.6	2	2	8279	8123
16,000	26.7	19.0	640	457.1	2	4	16,319	16,250-16,310
40,000	60	--	1440	--	3	--	40,600	--

Two variables were calculated to assess changes in bone's biomechanical properties throughout the postmortem interval: water and collagen. Water loss was estimated by weighing the bones before placement in the oven and after removal. Post-heat weight was subtracted from pre-heat weight. This value was used to calculate the percentage of total weight lost and approximate the water loss percentage. A one-centimeter axial section was cut from the proximal end of each femur and sent to the Mayo Clinic Biomaterials and Histomorphometry Core Laboratory for collagen analysis. Collagen samples were harvested as close to the time of fracture as possible to approximate collagen percentage at the time of the fracture and assess the role collagen plays in bone failure and fracture surface appearance. Additionally, after noting considerable inter-individual variation in collagen percentage, seven samples were sectioned before and after heating to calculate the percentage of collagen lost during heating. A Masson-Trichrome-Goldner stain was used to stain Type I collagen after samples were processed using a three-week dehydration period

including a series of graded alcohols (70% to 95% to 100% ethanol alcohol). The samples were infiltrated for a two-week period in methyl methacrylate, followed by the polymerization process in a water bath. The samples were then sectioned with a microtome, and the ratio of mineralized to non-mineralized (i.e., collagenous) material in each sample was calculated using BioQuant Image Analysis System (BIOQUANT Image Analysis Corporation, Nashville, TN 37221).

Fracture Experiments

The femoral shafts were fractured at Arizona State University's Computational and Experimental Mechanics Research Facility using a Columbus McKinnon (CM) Drop Test Frame. A three-point bending setup with pin-to-pin support was used to approximate femoral fixation between the acetabular and knee joints in vivo. The same parameters were used to initiate each impact and control fracture energy across the experiment. However, inter-sample variability (e.g., bone density, cortical thickness, and shaft diameter) necessitated a drop height range of 150-300 mm. All tests started at 150 mm and increased by 50 mm increments until fracture was successful. Accelerometer and load cell data were collected from sensors on the three-point bending machine to calculate the fracture energy of each impact. Peak load and peak acceleration of the final test (successful fracture) was used for data analyses.

High-speed photography was used for each fracture experiment to verify failure in tension, compression, and shear and visualize fracture propagation. Fracture surface appearance varies when bone fails in tension versus compression [11], so this variable was documented and analyzed with NCORR open source 2D-DIC (Digital Image Correlation) MATLAB software [12]. Two- and three-dimensional (2D and 3D) Digital Image Correlation (DIC and Stereo DIC, respectively) was used to calculate stress and strain across the bony

surface during the fracture experiments, as well as displacement and location of failure (Figure 1). DIC is carried out by administering a speckle pattern to each sample via a painting procedure [13-15]. Speckle quality is important to the ultimate resolution of DIC. For this project, dot sizes ranged from 5-25 pixels, as speckles smaller than one pixel are too difficult for the software to track [15]. The DIC provided data on the magnitude and directionality of fractures and facilitated the visualization and quantification of the differences in biomechanical properties in bone at varying postmortem intervals.

Figure 1. Digital Image Correlation film from an unheated (perimortem) sample. Cool colors (low values) indicate increased compression loads while warm colors (higher values) indicate increased tension loads. Failure initiated in tension (Shyamsunder et al. 2022).

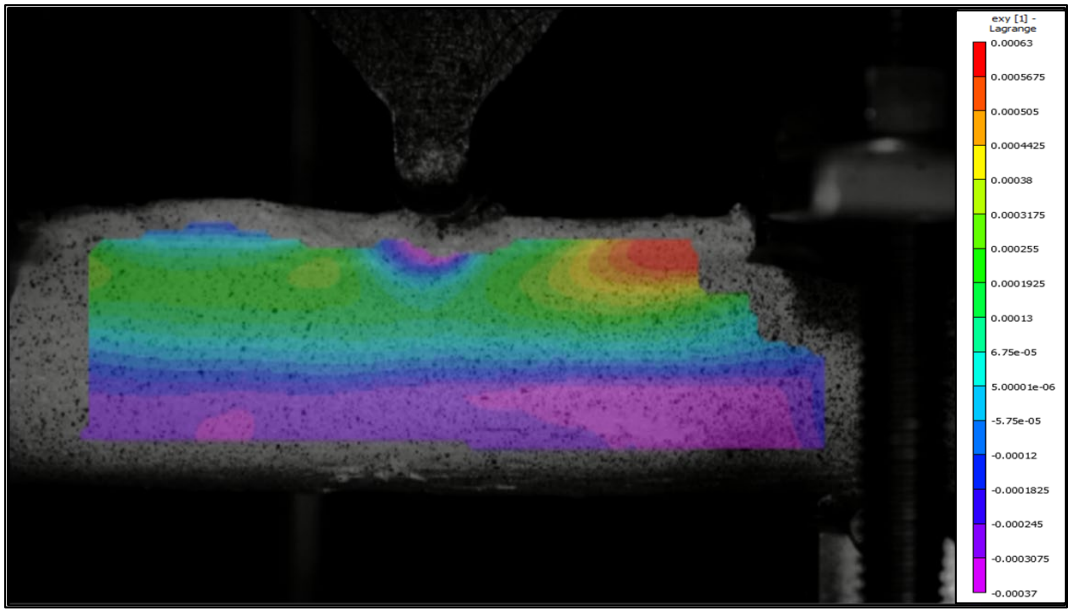

Scanning Electron Microscopy (SEM)

Knowledge of the histological features of bone on scanning electron micrographs is central to understanding the methods and outcomes of this research. Figure 2A shows an SEM image of a typical osteon with labeled features. The organizational structure of collagen fibers between the lamellae of osteons confers a unique mechanical advantage that makes bone the most biomechanically resilient human tissue [16-20]. These circumferential lamellae provide enhanced cross-sectional area of individual osteons [21], while collagen I fibers

provide elasticity that enables them to stave off mechanical failure [21-24].

Scanning electron micrographs were collected from the primary tension zones of each fracture, as determined by the high-speed photography and DIC analysis. A region of interest was defined within the center of the primary tension zone, and three microscopic fracture characteristics were scored: osteon pullout, osteon delamination, and microfractures. **Osteon pullout** occurs when substantial force deforms the lamellar structure of osteons to release stress, resulting in a pulled-out appearance to osteons viewed with SEM. Osteon pullout gives the osteon a "telescoped" appearance (Figure 2B). At later postmortem intervals, osteon pullout is compromised, and osteons are sheared flat. Collagen fiber bundles undergo considerable deformation before breaking, consistent with the behavior of a ductile material. However, **delamination** occurs when bone loses elasticity, causing the collagen fibers to have a low deformation threshold. When a critical degree of deformation is reached, the dry matrix breaks, and the collagen fibers snap, creating a delaminated appearance to lamellae (Figure 2C). **Microfractures** occur due to multiple failures in the brittle material with increasing PMI and elasticity loss, particularly along cement lines (Figure 3D).

Statistical Analysis

Pearson's correlation tests were used to test the relationships between ADH, water loss, collagen percentage, donor age, fracture energy variables (peak load and peak acceleration), and microscopic fracture characteristics. Multiple linear regression was used to examine the relationships between osteon pullout, delamination, microfractures and ADH, water loss, and collagen percentage. Multiple linear regression was also used to examine if energy required for failure was affected by ADH, water loss, collagen percentage, and/or donor age. All analyses were performed using R (version 4.2.1) and R Studio (version 2.3.492) software.

Figure 2. SEM images of osteons showing a normal osteon (A) and osteons exhibiting microscopic characteristics of fracture surfaces (B-D).

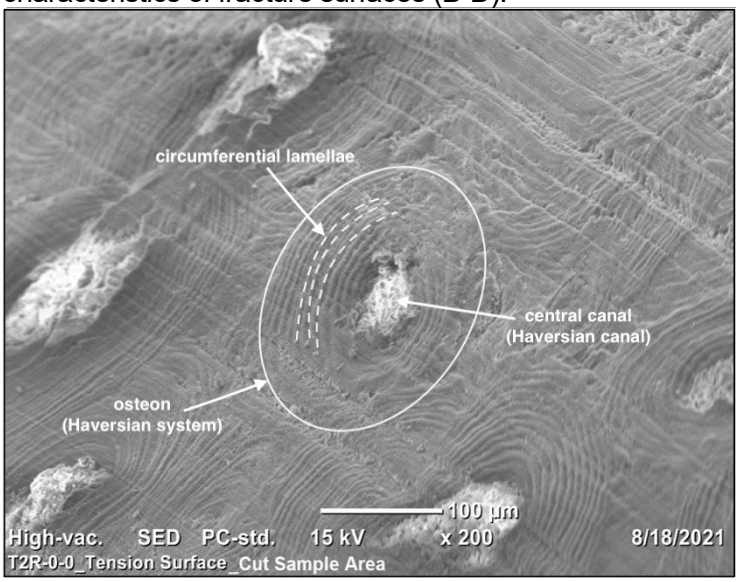

(A) Osteons visible on a cut surface of bone. Magnification=200X. These osteons lack pullout, delamination, and microfractures.

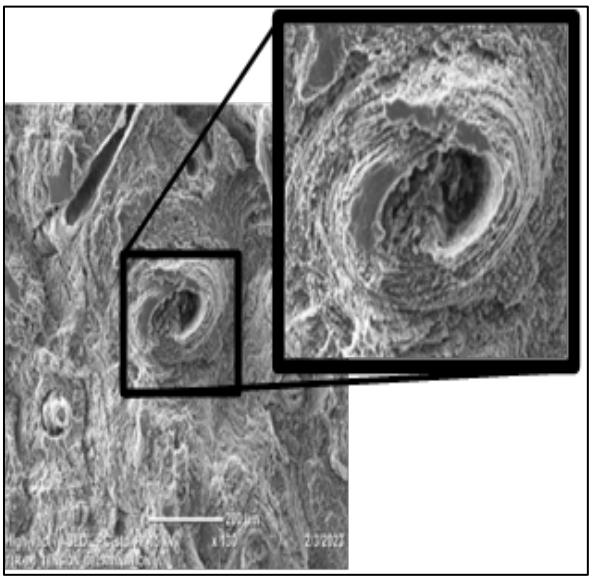

(B) Osteon pullout. Magnification=300X. Note the "telescoped" appearance of the osteon.

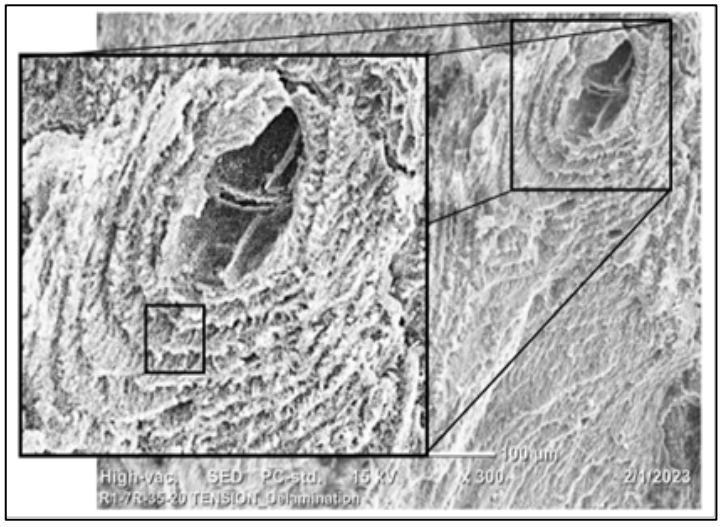

(C) Delamination. Magnification=300X. Collagen fiber bundles in elastic bone undergo considerable deformation before breaking, as visualized between the lamellae in this osteon.

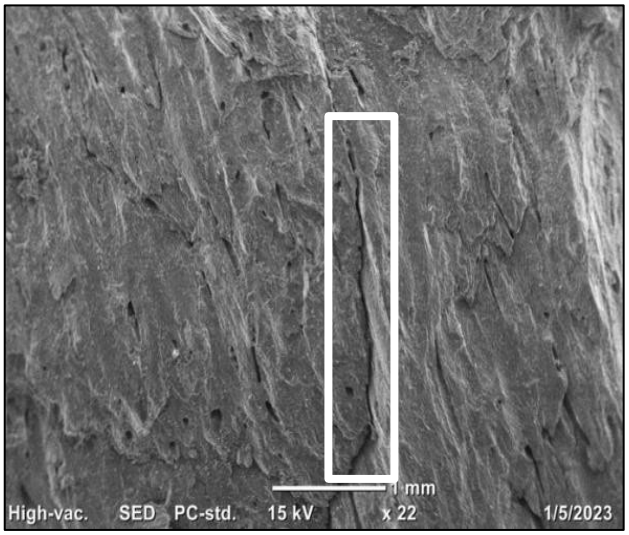

(D) Microfracture indicated by the box in the middle of this image. Magnification=22X.

Expected Applicability of the Research

This research demonstrates that microscopic fracture analysis is a more precise and reliable method for differentiating perimortem from postmortem traumatic events in bone.

This resource was prepared by the author(s) using Federal funds provided by the U.S. Department of Justice. Opinions or points of view expressed are those of the author(s) and do not necessarily reflect the official position or policies of the U.S. Department of Justice.

Being able to distinguish perimortem from postmortem events can mean the difference between the conviction of a perpetrator or an unsolved homicide. Any laboratory with access to a scanning electron microscope, which is standard equipment in crime laboratories, can utilize this method to assess fracture surfaces.

Participants and Other Collaborating Organizations

Participants

1. Natalie Langley, Principal Investigator

   Dr. Langley performed work in grant management, research design, collaboration with partner organizations, supervision of grant personnel, training and mentoring of the postdoctoral fellow, and report writing.

2. Jessica Skinner, Postdoctoral Research Fellow

   Dr. Skinner performed work in the areas of lab management, experimental protocols, data collection and management, research experiments, and personnel supervision (undergraduate research assistant). Dr. Skinner worked with Dr. Langley and the research team to process manuscript publications and disseminate results.

3. Subramaniam D. Rajan and Peter Goguen, Collaborators

   Dr. Rajan and Mr. Goguen designed and fabricated a modified test fixture to support the bone specimens, calibrated the drop frame system, performed impact tests, and collected data. Used three-dimensional (3D) digital image correlation (DIC) to calculate stress and strain across the bony geometry during the fracture experiments, as well as displacement and location of failure.

4. David Lott, Collaborator

   Dr. Lott provided access to laboratory equipment (see below) and mentored the PI regarding research and grant administration at Mayo Clinic Arizona.

5. Yuktha Shanavas, Undergraduate Research Assistant

   Ms. Shanavas processed SEM samples of bone and collected SEM images from fracture surfaces. She also assisted with the preparation of abstracts and conference presentations.

Collaborating Organizations

1. **Mayo Clinic Arizona**

   Mayo Clinic Arizona was the lead organization on this grant and provided access to equipment, laboratory space, software, and support personnel. The Lott Laboratory provided access to a laboratory in the Mayo Clinic Collaborative Research Building, Scottsdale, Arizona. The Lott Laboratory has the following equipment imperative for this effort: Leica EM CPD300 Critical Point Dryer, Leica EM ACE200 Sputter Coater, and JEOL JCM-6000Plus SEM. The lab has a password-protected computer with software dedicated to the JEOL SEM. Benchtop laboratory equipment in the lab includes pipettes, vortex mixer, precision scale, stir plate, graduate cylinders, glassware and MilliQ water system. The lab also provided biohazard disposal and flammable cabinet space to store flammable chemicals. The Center for Procedural Innovation provided space in the Collaborative Research Building to store the oven, cooler space for bone samples, and space to cut bone samples. The Langley Laboratory provided bench space in the Collaborative Research Building to prepare and store experimental samples and supplies, as well as bench space for the postdoctoral research fellow and undergraduate trainee.

2. **Mayo Clinic Rochester**

   The Mayo Clinic Biomaterials and Histomorphometry Core Laboratory provided the equipment and technical expertise to perform plastic and paraffin embedding of

biomaterials and to process and evaluate human bone tissue for the collagen analyses. The core is under the Directorship of Michael J. Yaszemski, M.D., Ph.D. and the Co-Directorship of Avudaiappan (Avudai) Maran, Ph.D. Dr. Yaszemski provided expertise in the disciplines of surgery and chemical and tissue engineering and biomaterials. The core is managed by James Herrick, MSA who has a background in biology, chemistry, histology, and business administration.

3. **Arizona State University**

The ASU Structural Mechanics Laboratory is a facility for full scale structural testing, model testing, stress analysis, and material property determination of various materials, systems, and structures. The lab conducted the fracture tests using the following test equipment:

1. Columbus McKinnon (CM) Drop Test Frame for fracture impacts
2. Video equipment for high-speed testing: Two Vision Research Phantom VRI-v7.3-8912MM cameras facilitating 3D analysis, 6688 fps at 800 x 600 resolution (3 gigapixels per second)
3. Video equipment for low-speed testing: Two 5-megapixel cameras to obtain digital images
4. Correlated Solution Inc.'s VIC3D software system to calculate 3D displacement and strain tensor field can be used with different test frames

Changes in Approach from Original Design

The project design had been tested and honed from a preliminary research project funded by the American Academy of Forensic Sciences (Forensic Sciences Foundation Lucas Grant); consequently, minimal changes were required from the design proposed in the grant

submission. However, one noteworthy change concerned the collagen analysis. After processing and analyzing 30 collagen samples, the Mayo Clinic Biomaterials and Histomorphometry Core Laboratory noted considerable inter-individual variation in collagen content. As a result, we began processing pre- and post-heat collagen samples to calculate a percentage of change in collagen content instead of a single estimate of the collagen content. While the point estimate allows us to quantify bone elasticity, we recognized we could not make inferences about postmortem changes in the collagenous proteins. This delta value is important to understanding the role collagen plays in bone elasticity and failure mechanics at varying time points during the postmortem interval, and we have incorporated this change into our research protocol moving forward.

Outcomes

Activities and Accomplishments

This grant has generated a number of activities and accomplishments detailed throughout this report. We have developed robust and replicable protocols for SEM imaging of bone fracture surfaces and histochemical analysis of Type I collagen in bone. Results of the research have been disseminated as conference presentations and manuscripts, as well as a media story highlighting the multidisciplinary collaboration across academic and medical institutions. Further, the project has advanced the careers of women in STEM. The postdoctoral research fellow (Dr. Jessica Skinner) has received a promotion to Senior Research Fellow at Mayo Clinic Arizona and has initiated funded collaborations in regenerative medicine research at Mayo Clinic. The undergraduate research fellow (Yuktha Shanavas) received early admission to medical school and continues to seek mentorship from Dr. Skinner and Dr. Langley. The research also investigated the utility of forensic fractography of bone (a new method of analyzing bone fracture surfaces) into the postmortem interval;

these results were disseminated to the forensic science community in a *Journal of Forensic Sciences* manuscript [25].

Results and Findings

Scanning electron microscopy (SEM) is an effective means of assessing microscopic surface characteristics of experimentally induced fractures in human bone at various postmortem intervals (PMIs). Microscopic fracture characteristics, including delamination, osteon pullout, and microfractures, differ as bone's material properties (e.g., elasticity and toughness) change throughout the PMI, elucidating perimortem and postmortem events more reliably than macroscopic analyses. Microscopic analysis of fracture surfaces is more reliable and sensitive for detecting biomechanical effects of decreased elasticity than macroscopic analysis. These factors make SEM analysis of bone fracture surfaces a promising avenue for refining fracture timing assessments.

Multiple linear regression showed that a model with ADH ($p = 0.77$), water loss ($p = 0.87$), donor age ($p = 0.93$), and collagen percentage ($p = 0.02$) did not significantly predict energy required for failure [$F(4, 25) = 2.24$, $p = 0.094$, $R^2 = 0.15$]. The only variable that added statistically significantly to the prediction was collagen percentage, highlighting the role that collagen plays in imparting elasticity and toughness to bone.

Multiple linear regression showed that osteon pullout, delamination, and microfractures are strong predictors of ADH and water loss but are weak predictors of collagen percentage (Table 2). Pearson's correlation demonstrated that collagen percentage does not correlate with ADH ($r=0.01$; p 0.98; 95% confidence interval: -0.33, 0.35), but water loss has a strong positive correlation with ADH ($r=0.91$; $p<.001$; 95% confidence interval: 0.82, 0.96), with samples losing between 2 and 20% of total bone weight, depending on length of time in the oven and temperature (Figure 3). These results suggest the most significant impact on

elasticity in the early PMI is water loss, not collagen content. The reason may be that the namely the release of water as they hydrophilic glycosaminoglycans (GAGs) undergo break down earlier than Type I collagen, releasing the GAG-bound water at a faster rate than collagen degradation . When GAGs become compromised, water leaches out of the extracellular matrix, affecting the structural integrity of collagen and increasing the elastic modulus [26-30].

Osteon pullout decreased significantly with increased ADH (r= -0.91 | p<.001 | 95% confidence interval: -0.95, -0.83) and water loss (r= -0.82 | p<.001 | 95% confidence interval: -0.91 -0.66) (Figure 4). Osteon pullout is most prevalent in the early PMI, and this feature indicates elasticity in the bone matrix. In fact, osteon pullout is significantly correlated to PMI even in the absence of microfractures. Delamination increased significantly with increased ADH (r= 0.91 | p<.001 | 95% confidence interval: 0.83, 0.96) and water loss (r= 0.82| p<.001| 95% confidence interval: -0.91 -0.66) (Figure 5). Delamination becomes more prevalent as bone elasticity is compromised with increasing PMI. Microfractures also increased with higher ADH (r= 0.84 | p<.001 | 95% confidence interval: 0.70, 0.92) and water loss (r= 0.78| p<.001| 95% confidence interval: 0.59, 0.86) (Figure 6).

These results demonstrate that, due to the complex microstructure of bone, histologic images provide more information about fracture timing than macroscopic analyses and may improve the accuracy and resolution of fracture timing estimates [6, 7, 11, 31-38].

Table 2. Multiple linear regression results showing the relationships between microscopic fracture characteristics (osteon pullout, delamination, microfractures) and three dependent variables: ADH, water loss, and collagen percentage.

Dependent Variable: Accumulated Degree Hours (ADH)				
Independent variables	R^2	Adjusted R^2	F-statistic, (DF)	p value
• Osteon Pullout • Delamination • Microfractures	0.91	0.90	95.29, (3, 30)	<0.001

Dependent Variable: Water Loss				
Independent variables	R^2	Adjusted R^2	F-Statistic, (DF)	p value
• Osteon Pullout • Delamination • Microfractures	0.74	0.71	26.23, (3, 28)	<0.001

Dependent Variable: Water Loss				
Independent variables	R^2	Adjusted R^2	F-Statistic, (DF)	p value
• Osteon Pullout • Delamination • Microfractures	0.14	0.0	1.67, (3, 30)	0.19

Figure 3. Association between ADH and organic components of bone (collagen and water).

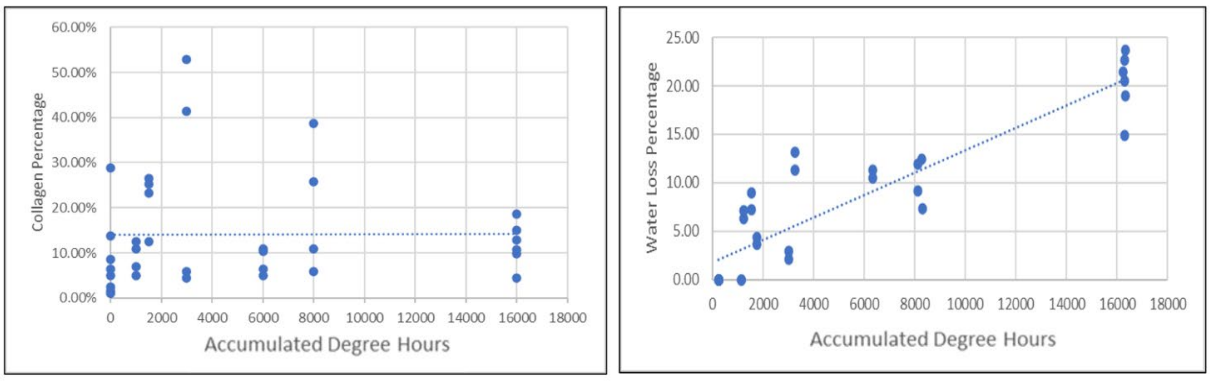

This resource was prepared by the author(s) using Federal funds provided by the U.S. Department of Justice. Opinions or points of view expressed are those of the author(s) and do not necessarily reflect the official position or policies of the U.S. Department of Justice.

Figure 4. Association between osteon pullout versus ADH and water loss.

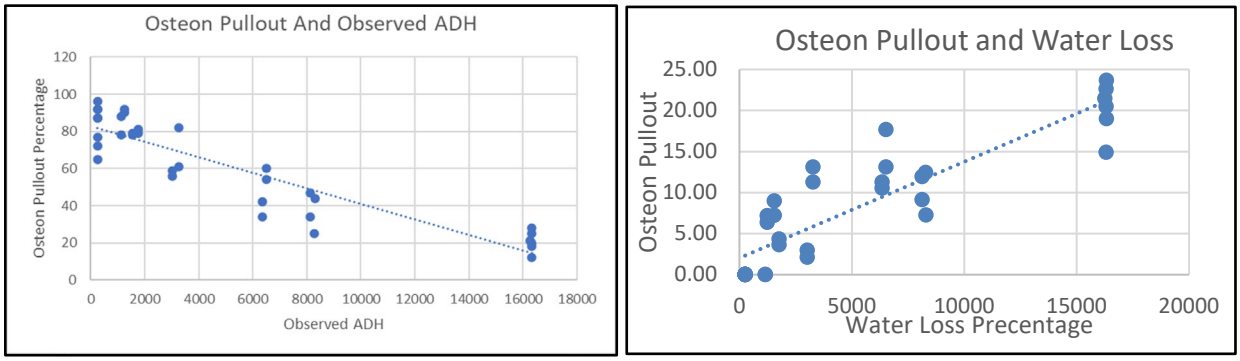

Figure 5. Association between delamination versus ADH and water loss.

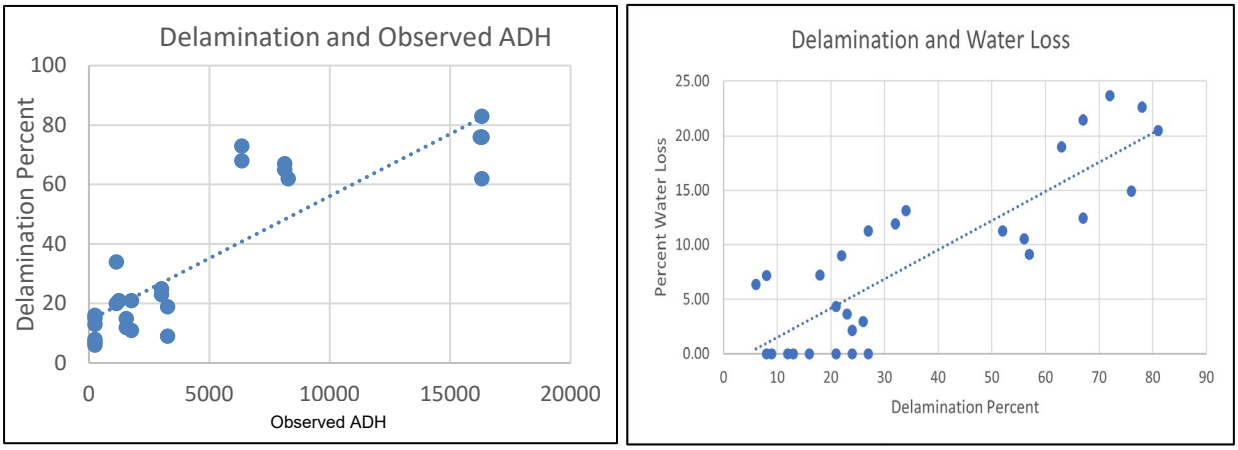

Figure 6. Association between microfractures versus ADH and water loss.

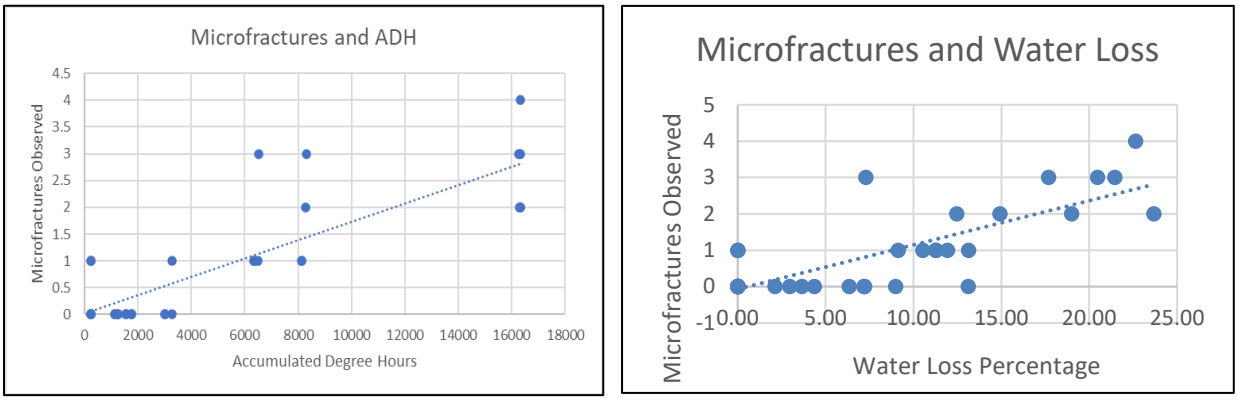

This resource was prepared by the author(s) using Federal funds provided by the U.S. Department of Justice. Opinions or points of view expressed are those of the author(s) and do not necessarily reflect the official position or policies of the U.S. Department of Justice.

Limitations

Power analysis suggests small sample size is the primary limiting factor to broadening our conclusions. A larger sample is needed to increase statistical power and address sample gaps in the ADH timeline. Additionally, extending the PMI may elucidate the roles of extracellular matrix water versus collagen regarding microscopic fracture feature expression throughout the PMI. We found that collagen is retained in early PMI, but postmortem water loss affects elasticity considerably. We hypothesize collagen degradation will play a greater role in fracture surface feature expression with increasing ADH. Next steps for calibrating these data include the proposed bone mineral density study, additional collagen analyses, and automating data collection from the SEM images with machine learning software. We are also conducting interobserver error studies and method validation.

Artifacts

List of products

1. **Publications**

   Skinner, J., Langley, N., Joseph, M., Herrick, J., Brown, R., Waletzki, B., Goguen, P., Shyamsunder, L. and Rajan, S., 2023. Do bone elasticity and postmortem interval affect forensic fractographic analyses? *Journal of Forensic Sciences*.

   https://doi.org/10.1111/1556-4029.15237

   https://onlinelibrary.wiley.com/doi/full/10.1111/1556-4029.15237

2. **Manuscripts in Preparation**

   Skinner, J., Langley, N., Shanavas, Y., Joseph, M., Herrick, J., Brown, R., Waletzki, B.,

Goguen, P., Shyamsunder, L. and Rajan, S., 2023. The Microscopic Characteristics of Peri- and Postmortem Fracture Surfaces.

3. Conference Presentations

American Academy of Forensic Sciences 75th Annual Meeting

Oral Presentation: The Microscopic Characteristics of Peri- and Postmortem Fracture Surfaces

Jessica Skinner; Natalie Langley; Malin Joseph; Yuktha Shanavas; Brian Waletzki; Robert Brown; James Herrick; Peter Goguen; Loukham Shyamsunder; Subramaniam Rajan

https://www.aafs.org/sites/default/files/media/documents/2023Proceedings_FINAL-june-1-23.pdf

American Academy of Forensic Sciences 74th Annual Meeting

Oral Presentation: Do Bone Elasticity and Postmortem Interval Affect Forensic Fractographic Analyses?

Jessica Skinner; Natalie Langley; Malin Joseph; Brian Waletzki; Robert Brown; James Herrick; Peter Goguen; Loukham Shyamsunder; Subramaniam Rajan

https://www.aafs.org/sites/default/files/media/documents/2022Proceedings_Final.pdf

Data Archives

1. Data archived on a secure Mayo Clinic server
2. Tracking data for samples hosted on LabGuru
3. Procedures and analytical protocols hosted on LabGuru

Data sets generated

1. Vital statistics data
2. Fracture testing data

a. Acceleration and load cell
b. Fracture energy
c. Digital Image Correlation (DIC) data
d. High speed videos of 3-point bending fracture events

3. Fractographic assessment data (fractographic scores of fracture surfaces)
4. Photos of fractured specimens
5. Digitally scanned histologic slides stained for collagen I proteins
6. Bioquant image analysis of histologic slides
7. Scanning electron microscope images

Dissemination activities

In addition to the list of products above, the PI and ASU collaborators were interviewed for a media story about this interdisciplinary research project. Stephen Filmer, a journalist with Arizona State University's Media Relations and Strategic Communications produced a story about for *Catalyst*. Catalyst explores research at Arizona State University and its impact on the world. The show is supported by ASU's BioDesign Institute, College of Liberal Arts and Sciences, Fulton Schools of Engineering, Global Futures Laboratory, Global Security Initiative, Interplanetary Initiative, and Knowledge Enterprises. The full media story is available here: https://news.asu.edu/colleges-and-units/mayo-clinic.

References Cited

1. Cappella A, Amadasi A, Castoldi E, Mazzarelli D, Gaudio D, Cattaneo C. The difficult task of assessing perimortem and postmortem fractures on the skeleton: A blind text on 210 fractures of known origin. Journal of Forensic Sciences. 2014;59(6):1598-601.
2. Cappella A, Cattaneo C. Exiting the limbo of perimortem trauma: A brief review of microscopic markers of hemorrhaging and early healing signs in bone. Forensic Sci Int. 2019 Sep;302:109856.
3. Coelho L, Cardoso HFV. Timing of blunt force injuries in long bones: The effects of the environment, PMI length and human surrogate model. Forensic Science International. 2013;233(1-3):230-7.
4. Efe JOJ, Igho OE, Mamuyovwi UJ. Investigating antemortem, perimortem and postmortem injuries: forensic implication. Bangladesh Journal of Medical Science. 2021;20(1):50-7.
5. Kemp WL. Postmortem Change and its Effect on Evaluation of Fractures. Academic Forensic Pathology. 2016;6(1):28-44.
6. Pechníková M, Porta D, Cattaneo C. Distinguishing between perimortem and postmortem fractures: are osteons of any help? Int J Legal Med.2011; 125(4):591-5.
7. Wescott DJ. Postmortem change in bone biomechanical properties: Loss of plasticity. Forensic Science International. 2019;300:164-9.
8. Wheatley BP. Perimortem or postmortem bone fractures? An experimental study of fracture patterns in deer femora. Journal of Forensic Sciences. 2008;53(1):69-72.
9. Wieberg DAM, Wescott DJ. Estimating the timing of long bone fractures: Correlation between the postmortem interval, bone moisture content, and blunt force trauma fracture characteristics. Journal of Forensic Sciences. 2008;53(5):1028-34.
10. Bozec L, Odlyha M. Thermal denaturation studies of collagen by microthermal analysis and atomic force microscopy. Biophysical Journal. 2011;101(1):228-36.
11. Braidotti P, Branca FP, Stagni L. Scanning electron microscopy of human cortical bone failure surfaces. Journal of Biomechanics. 1997;30(2):155-62.
12. Blaber J, Adair B, Antoniou A. Ncorr: Open-Source 2D Digital Image Correlation Matlab Software. Experimental Mechanics. 2015;55(6):1105-22.
13. Shyamsunder L, Khaled B, Rajan SD, Pereira JM, DuBois P, Blankenhorn G. Numerical validation of composite panel impact tests. International Journal of Impact Engineering. 2022;159:104032-.
14. Khaled BM, Shyamsunder L, Holt N, Hoover CG, Rajan SD, Blankenhorn G. Enhancing the predictive capabilities of a composite plasticity model using cohesive zone modeling. Composites Part A: Applied Science and Manufacturing. 2019;121:1-17.
15. Sutton MA, Matta F, Rizos D, Ghorbani R, Rajan S, Mollenhauer DH, et al. Recent Progress in Digital Image Correlation: Background and Developments since the 2013 W M Murray Lecture. Experimental Mechanics. 2017;57(1):1-30.
16. Hart NH, Nimphius S, Rantalainen T, Ireland A, Siafarikas A, Newton R. Mechanical basis of

bone strength: influence of bone material, bone structure and muscle action. Journal of musculoskeletal & neuronal interactions. 2017;17(3):114.
17. Andronowski JM, Crowder C, Soto Martinez M. Recent advancements in the analysis of bone microstructure: New dimensions in forensic anthropology. Forensic Sciences Research. 2018;3(4):278-93.
18. Ascenzi A, Benvenuti A. Orientation of collagen fibers at the boundary between two successive osteonic lamellae and its mechanical interpretation. In: Biomech J, editor. Princeton: Princeton University Press; 1986;455-63.
19. Ascenzi A, Bonucci E. The tensile properties of single osteons. The Anatomical Record. 1967;158(4):375-86.
20. Casari D, Michler J, Zysset P, Schwiedrzik J. Microtensile properties and failure mechanisms of cortical bone at the lamellar level. Acta Biomaterialia. 2021;120:135-45.
21. Bernhard A, Milovanovic P, Zimmermann EA, Hahn M, Djonic D, Krause M, et al. Micro-morphological properties of osteons reveal changes in cortical bone stability during aging, osteoporosis, and bisphosphonate treatment in women. Osteoporos Int. 2013 Oct;24(10):2671-80.
22. Chen Y, Wang W, Li X. Fracture analysis of cortical bone under the condition of cement line debonding and osteon pullout. International Journal of Biomathematics. 2018;11(02):1850023.
23. Green AE, Jj S, Schultz JJ. An Examination of the Transition of Fracture Characteristics in Long Bones from Fresh to Dry in Central Florida: Evaluating the Timing of Injury. In: Sci JF, editor. Cambridge: 2003.
24. Hiller LP, Stover SM, Gibson VA, Gibeling JC, Prater CS, Hazelwood SJ, et al. Osteon pullout in the equine third metacarpal bone: Effects of ex vivo fatigue. Journal of Orthopaedic Research. 2003;21(3):481-8.
25. Skinner J, Langley N, Joseph M, Herrick J, Brown R, Waletzki B, et al. Do bone elasticity and postmortem interval affect forensic fractographic analyses? Journal of Forensic Sciences. 2023.
26. Ambrock K, Grohe B, Mittler S. Controlling the hydrophilicity and cohesion during deposition of highly oriented type I collagen films: An approach for biomedical applications. Thin Solid Films. 2018;656:75-82.
27. Bi Y, Patra P, Faezipour M. Structure of collagen-glycosaminoglycan matrix and the influence to its integrity and stability. 2014 36th Annual International Conference of the IEEE Engineering in Medicine and Biology Society, EMBC 2014. 2014:3949-52.
28. Bonicelli A, Di Nunzio A, Di Nunzio C, Procopio N. Insights into the Differential Preservation of Bone Proteomes in Inhumed and Entombed Cadavers from Italian Forensic Caseworks. Journal of Proteome Research. 2022;21(5):1285-98.
29. Rho JY, Pharr GM. Effects of drying on the mechanical properties of bovine femur measured by nanoindentation. Journal of materials science Materials in medicine. 1999;10(8):485-8.
30. Brazda IJ, Reeves J, Langohr GDG, Crookshank MC, Schemitsch EH, Zdero R. Biomechanical

properties and thermal characteristics of frozen versus thawed whole bone. https://doiorg/101177/0954411920929455. 2020;234(8):874-83.
31. Braidotti P, Bemporad E, D'Alessio T, Sciuto SA, Stagni L. Tensile experiments and SEM fractography on bovine subchondral bone. J Biomech. 2000; 33(9):1153-7.
32. Cattaneo C, Cappella A, Cunha E. Post Mortem Anthropology and Trauma Analysis. P5 Medicine and Justice: Innovation, Unitariness and Evidence. 2017;166-79.
33. Hentschel K, Wescott D, editors. Differentiating peri-mortem from postmortem blunt force trauma by evaluating fracture tension surface topography using geographic information systems. Proceedings of the 67th Annual Scientific Meeting of the American Academy of Forensic Sciences; 2015; Colorado Springs, CO, USA: . American Academy of Forensic Sciences.
34. Evans FG, Vincentelli R. Relations of the compressive properties of human cortical bone to histological structure and calcification. Journal of Biomechanics. 1974;7(1):1-2.
35. Gaziano P, Monaldo E, Falcinelli C, Vairo G. Elasto-damage mechanics of osteons: A bottom-up multiscale approach. Journal of the Mechanics and Physics of Solids. 2022;167:104962.
36. Gerstenfeld LC, Wronski TJ, Hollinger JO, Einhorn TA. Application of histomorphometric methods to the study of bone repair. Journal of Bone and Mineral Research. 2005;20(10):1715-22.
37. Tersigni MTA. Frozen human bone: A microscopic investigation. Journal of Forensic Sciences. 2007;52(1):16-20.
38. Cattaneo C, Andreola S, Marinelli E, Poppa P, Porta D, Grandi M. The Detection of Microscopic Markers of Hemorrhaging and Wound Age on Dry Bone: A Pilot Study. The American Journal of Forensic Medicine and Pathology.2010; 31(1):22-6.